The future prospects for SiPM based receivers for visible light communications.

Long Zhang, Hyunchae Chun, Zubair Ahmed, Grahame Faulkner,
Dominic O'Brien, *Member IEEE,* and Steve Collins, *Member IEEE.*

***Abstract*— A silicon photomultiplier (SiPM) could be used to create visible light communications receivers whose sensitivity is determined by shot-noise. However, its finite output pulse width will limit its bandwidth and its recovery time and dark count rate could limit its sensitivity. In this paper, a method of accurately determining the signal levels needed to transmit data in a shot-noise limited system using PAM is described. In addition, a method of estimating the additional power needed to use equalisation to overcome inter-symbol interference caused by the finite output pulse width of SiPMs is described. The best way to achieve more than 1 Gbps with this type of receiver and how to select the best available SiPM as a receiver are then discussed.**

***Index Terms*—** SPAD, APD, VLC, SPAD-based receivers, Visible light communication, optical wireless communication

I. Introduction

The increasing demand for indoor radio frequency wireless communications capacity has stimulated interest in using other parts of the electromagnetic spectrum for wireless communications. Ideally, this alternative spectrum would be unlicensed and provide a high data rate. For these reasons, there has been a rapidly growing interest in employing the visible part of the electromagnetic spectrum for wireless communications [1-3].

The overall capacity of any visible light or optical wireless communications channel will be partly determined by the signal to noise ratio of the received signal. Consequently, some receivers incorporate an avalanche photodiode (APD) that amplifies the detected signal using avalanche multiplication. Unfortunately, this process also generates excess shot noise in the APD and this reduces the maximum available signal to noise ratio. An alternative method of increasing the signal to noise ratio of a receiver is to operate an APD above its breakdown voltage and place it in series with a quenching device, such as a resistor, to create a single photon avalanche diode (SPAD) [4,5]. Results obtained using optical receivers that incorporate arrays of SPADs (now known as silicon photomultipliers (SiPMs)) have been previously reported [6-10]. More recently, it has been suggested that receivers containing SiPMs will be more sensitive than receivers containing APDs if the photon detection efficiency (PDE) of the SiPM is higher than 14% [11].

L.Zhang, H. Chun, Z. Ahmed, G. E. Faulkner, D. C. O'Brien and S.Collins are with the Department of Engineering Science, University of Oxford, Oxford, UK. e-mail:{long.zhang, grahame.faulkner, dominic.obrien, steve.collins}@eng.ox.ac.uk. This research work was supported by the EPSRC Programme Grant "Super Receivers for Visible Light Communications" (EP/R00689X/1). H. Chun is now with the Department of Information and Telecommunication, Incheon National University, Incheon, Korea. e-mail: hyunchae.chun@inu.ac.kr.

As a result of continuing improvements in manufacturing processes, SiPMs are now available with PDEs significantly higher than 14%. Incorporating these devices rather than an APD in a receiver is therefore expected to improve the sensitivity of the receiver. However, SiPMs are available with different active areas, PDEs and number of individual SPADs per unit area. This means that a receiver designer has to be able to select a particular type of SiPM from those that are available and estimate the performance of a receiver containing the selected SiPM. In addition, if SiPMs become an integral part of VLC receivers, their manufacturers will be interested in optimising their performance for this large potential market. To help future SiPM and receiver designers this paper describes various non-ideal aspects of SiPM behaviour and ways to determine their impact on the performance of VLC receivers that incorporate a SiPM.

Section II introduces the SiPM used in experiments and the results of experiments to determine the impact of recovery time on the linearity of this device. Section III then contains a description of the calculation of the signal levels needed for 4 PAM when the dominant noise source is shot (Poisson) noise. Results that demonstrate the accuracy of these calculations are presented in section IV. The results of experiments to determine the impact of the finite output pulse width of SiPMs are described in Section V. In section VI the relative merits of achieving data rates of more than several hundred Mbps using OOK and PAM are discussed. The method developed to quantify the effects of recovery time, dark counts and the width of output pulses on the signal intensity needed to transmit data is then described in Section VII. The results obtained using this method to predict the performance of a SiPM receiver are presented in section VIII. Conclusions are drawn in section IX.

II. Characterisation of the SiPM

The impacts of the recovery time, dark counts and finite output pulse width of an SiPM have been investigated using a S12571-010C SiPM [12] within a C11209-110 Multi-Pixel Photon counter (MPPC). The SiPM in this MPPC uses passive

Table I Parameters for the C11209-110 MPPC which incorporates a S12571-010C

Area	$1mm^2$
Pitch	10 µm
Number of SPADs	10^4
Fill Factor	33%
Typical Dark Count Rate	100 kHz
Maximum Dark Count Rate	200 kHz
Amplifier Cut-Off Frequency	40 MHz

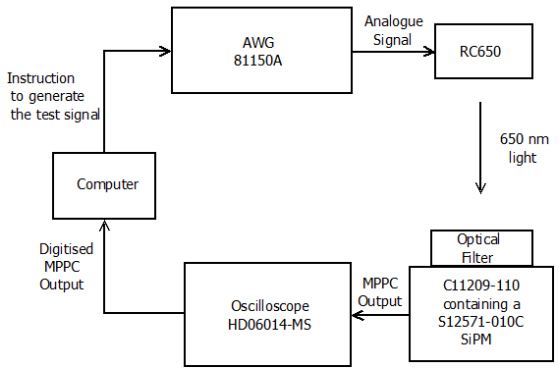

Fig.1. A schematic diagram of the experiment used to characterize the SiPM and transmit data to the SiPM.

quenching and a common output. In addition to the SiPM the MPPC contains a high speed amplifier that amplifies the signal from this common output. The critical performance parameters of the MPPC are listed in Table I.

Since each individual SPAD in a SiPM is inactive during its recovery time, the existence of a recovery time will lead to a non-linear SiPM response. The recovery time has therefore been measured using the experimental set-up, shown in the schematic diagram in Fig. 1, which was also used for data transmission experiments described later in this paper. The.light source used in this setup was a RC650 RCLED that emits 650 nm light. The signal emitted by this RCLED was determined by the voltage generated inside an Agilent 81150 arbitrary wave form generate (AWG) that was controlled by a computer. In order to reduce the effects of ambient light on subsequent data transmission experiments a 650 nm band-pass optical filter, with a 40 nm wide passband, was placed over the active area of the SiPM within the MPPC. A 12-bit oscilloscope, LeCroy HDO6014-MS, was then used to capture the output signal from the MPPC. Finally, the captured signal was processed offline within a computer.

To determine the impact of the recovery time on the SiPM response the optical power incident on the SiPM was varied. The average number of photons detected in 10 ns was then determined at each of these power levels. The results obtained from this experiment, Fig. 2, show the expected non-linear relationship between the measured output and the optical power falling on the active area of the SiPM. For VLC applications saturation of the SiPM response should be avoided and so Fig 2 shows the experimental results up to the optical power level at which saturation occurs.

Two models of the non-linear response of a SiPM have been described previously [13,14]. However, it has been shown that both models give similar results before saturation occurs[14] and so the simpler paralyzable model can be used to predict the response of an SiPM.

The impact of the SiPM recovery time on its response depends upon the rate at which photons arrive at the SiPM. For a SPAD with an area A_{SPAD} and photon detection probability, *PDP*, and light intensity *L*, with an average photon energy E_p, the rate of arrival of photons, λ_{in}, is

$$\lambda_{in} = \frac{L \times A_{SPAD} \times PDP}{E_p} \quad (1)$$

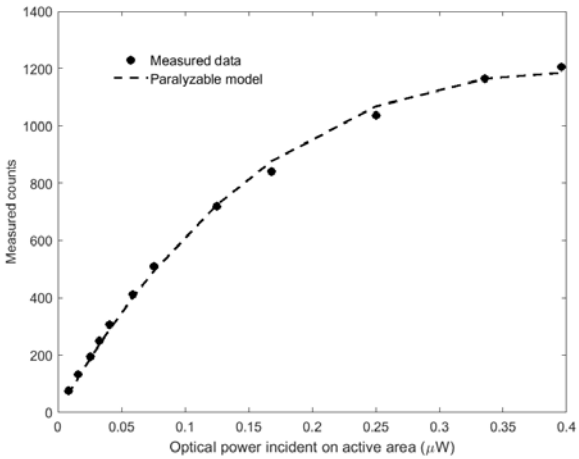

Fig.2. The measured effect of recovery time on the linearity of the MPPC compared to the paralyzable model of this effect.

The paralyzable model then predicts that for a recovery time τ_{total} the number of photons detected in time T is [14]

$$N_{out\_total} = N_{SPADs} T \lambda_{in} e^{-\lambda_{in} \times \tau_{\text{total}}} \quad (2)$$

where N_{SPADs} is the number of individual SPADs in the SiPM. The maximum count rate is then

$$C_{max} = \frac{N_{SPADs}}{\tau_{\text{total}} \times e} \quad (3)$$

In addition to the experimental results Fig. 2 shows the best fit of the paralyzable recovery time model to the data. This fit shows that the recovery time of this SiPM is 31 ns and its maximum count rate is 119 Gcounts/s. The results show that the non-linear response of the SiPM can be accurately predicted. In addition, the maximum count rate means that the ratio of the number of SPADs in a SiPM to their recovery time is an important performance parameter for VLC applications.

III. Calculation of PAM Signal Levels

A second non-ideality of SiPMs is the dark counts that are additional to any counts from ambient light which create a minimum background count rate. For a particular background count level several different combinations of PAM levels will achieve the same BER. The optimum choice of PAM symbol levels to achieve the highest sensitivity (i.e. the minimum number of photons per bit) have been found by calculating the BERs for more than 4500 possible combinations of PAM levels at different background counts per bit. The results in the second and third rows of Table II show that this exhaustive search leads to a set of levels with slightly fewer photons per bit than a previous limited search [15]. Furthermore, inspection of the distribution of errors in the best combinations of levels shows that the errors between neighbouring levels are typically at least 10 orders of magnitude larger than errors between other pairs of levels. This suggests that the overall BER can be reduced by using a Gray code rather than a simple binary code. A comparison of the third and fourth rows of Table II shows that the use of Gray coding results in a small reduction in the number of photons per bit.

Table II The average number of photons per bit needed to support 4 PAM in the presence of 4 levels of background counts per bit. Each row corresponds to a different method of calculating this average and/or the use of Gray coding of the two bits. (The numbers in brackets are the equivalent number of attoJoules per bit)

Background counts per bits	1	10	50	100
Photons per bits (limited search) [15]	24.2 (7.37)	39.6 (12.1)	81.1 (24.7)	122.6 (37.3)
Photons per bit (exhaustive search)	21.2 (6.46)	36 (11.0)	74.2 (22.6)	112.7 (34.3)
Photons per bits with Gray coding (exhaustive search)	20.3 (6.18)	34.6 (10.5)	72.2 (22.0)	110.3 (33.6)
Photons per bits with Gray coding (evenly distributed)	20.4 (6.21)	35.0 (10.7)	72.6 (22.1)	110.8 (33.7)

The distribution of errors also suggests that when Gray coding is used the 4 PAM BER is the sum of the BERs between neighbouring levels. The BER between two neighbouring levels is the same as the BER when these two levels are using in OOK. Furthermore, it has been observed that the BERs between neighbouring levels should be equal, which means that the BER between neighbouring levels should be one third of the BER for 4 PAM. An efficient strategy for finding good combinations of levels for 4 PAM is therefore to start with the lowest level represented by the number of background counts per bit. The higher OOK level that achieves the required BER between neighbouring levels is then calculated. This higher level is then the second PAM level which becomes the lower level when the third level is calculated. Finally the third level becomes the lower level and the final level for 4 PAM is calculated. As shown by the last two rows in Table II the differences between the results of the two methods of calculating the levels are approximately 1%. The differences are therefore smaller than the variations that are expected between the outputs of different laser diodes or LEDs. This simpler strategy of determining PAM levels therefore gives acceptable approximations to the optimum results.

Fig. 3 shows the 3 signal levels of 4 PAM required to maintain a target BER of 10^{-3} at different background counts per symbol time. Since for a SiPM the dominant noise source is proportional to the signal level the higher signal levels are more widely separated than the lower levels. In addition, all the symbol levels increase in response to an increasing number of background counts. Furthermore, their dependence upon background counts is similar to the equivalent results for OOK [11]. One observation from Fig 3 is that the impact of background count is negligible when the number of background counts within a symbol period is one fifth of the probability that no photons are detected within a symbol period when a 1 is transmitted. Most importantly, the results in Fig. 3 show that the number of photons per bit required to obtain a specific BER increases less rapidly than the number of background counts. This suggests that, if the number of background counts is dominated by ambient light, increasing the area of a SiPM will reduce the signal intensity (Wm^{-2}) needed to transmit data.

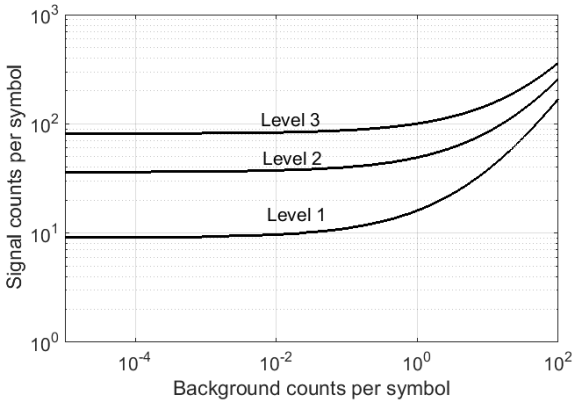

Fig. 3. The calculated number of detected pho tons per symbol needed to transmit the three highest levels of 4PAM at different numbers of background counts per symbol.

IV. Verification of 4 PAM Levels

The PAM levels in Fig 3 were calculating assuming that inter-symbol interference (ISI) caused by the finite width of the SiPM output pulses is negligible. In order to confirm the accuracy of the results in Fig 3 the 4 PAM levels needed to transmit 2 Mbps were determined experimentally. This relatively low data rate was chosen so that the symbol time, 1 µs, was much longer than the SiPM output pulse width, 10 ns, so that ISI is negligible.

The 4 PAM levels needed to transmit 2 Mbps with a BER of 10^{-3} have been determined using the experimental setup shown in Fig. 1. In these experiments the first step of the off-line processing was to synchronise the received signal with the transmitted signal. After synchronisation the number of detected photons within each symbol period was determined by summing the sampled signals in each symbol period. The resulting sum was then converted to an estimate of the corresponding number of photons by dividing the result by a constant that represented the summed signal from one photon. These photon counts were then converted to the corresponding 4 PAM symbols using optimum decision thresholds before the 4 PAM symbols were converted to a pair of bits. The result stream of bits was then compared to the transmitted bit stream so that the BER could be calculated.

The results in table III show that although photons are being counted the measured symbol levels are not those calculated assuming Poisson statistics. In fact, the highest symbol level is 17% higher than the estimated level. However, very accurate estimation of 4 PAM levels relies upon detailed knowledge of the noise associated with varying levels of optical power. The distributions of photon counts within 1 µs were therefore measured at 10 different light levels. The results of these experiments showed that the error functions that represented the measured data most accurately where

$$Pe(l-1|l,x) = \frac{1}{2} erfc\left(\frac{x-0.95*\mu}{0.75*\sigma\sqrt{2}}\right) \quad (4)$$

$$Pe(l+1|l,x) = \frac{1}{2} erfc\left(\frac{0.925*\mu-x}{1.25*\sigma\sqrt{2}}\right) \quad (5)$$

Table III A comparison of the estimated and measured numbers of photons per level and the average number of photons per bit needed to transmit 2 Mbps with a BER of 10^{-3} in the dark. (The numbers in brackets are the equivalent number of attoJoules)

	Level 1	Level 2	Level 3	Average
Measured number of photons per symbol	10.9 (3.32)	42.6 (13.0)	102 (31.1)	19.4 (5.91)
Photons per symbol predicted assuming Poisson noise	10.8 (3.29)	39.7 (12.1)	86.8 (26.4)	17.2 (5.24)
Photons per symbol predicted using (4) and (5)	11.0 (3.35)	41.9 (12.8)	99.6 (30.3)	19.1 (5.82)

where μ is mean of the photon counts distribution, σ is the standard deviation of the photon counts distribution and both 0.925 and 1.25 are fitting parameters.

The error functions in (4) and (5) determine the BERs when two light levels are used to transmit OOK data. These error functions can therefore be used to determine the optimum 4 PAM levels for this SiPM by evenly distrubuting errors between different pairs of PAM levels. The results obtained using (4), (5) and the efficient method of determining PAM levels described in section III are contained in the last row of Table III. A comparison of the second and fourth rows of this table shows that the measured symbol levels are within approximately 2% of the levels predicted using the measured error functions, (4) and (5). The proposed method of determining the signal levels required to transmit data using PAM is therefore accurate, and can be very accurate if the error functions of the link are characterised in detail.

V. IMPACT OF OUTPUT PULSE WIDTH

The last important non-ideality of SiPMs is their finite output pulse width, which will create ISI when 4 PAM is used to transmit data rates that are significantly higher than current WiFi data rates to individual users. For example, when 4 PAM is used to transmit 200 Mbps the symbol time is shorter than the duration of the MPPC output pulse and ISI will occur. The eye diagram in Fig. 4(a) shows that without equalisation the eye is almost closed. To achieve the target BER, the impact of the ISI was therefore mitigated using a DFE equalizer [16]. The eye diagram of the equalised 4 PAM data, Fig. 4(b), confirms that equalisation opens the eye. These results also show that the increased noise in the higher PAM levels means that the higher levels have to be more widely spaced, which means that the vertical eye opening is larger between the higher levels.

The equalization technique used to open the eye employs multiple samples of the signal and it therefore increases the effective noise in the signal. To overcome this additional noise there is a power penalty associated with using equalization. This power penalty is the ratio of the power per bit needed to use equalization when ISI occurs to the power per bit that would have been required if ISI didn't occur. The power penalty required to compensate for ISI when using 4 PAM to transmit 200 Mbps has been estimated numerically.

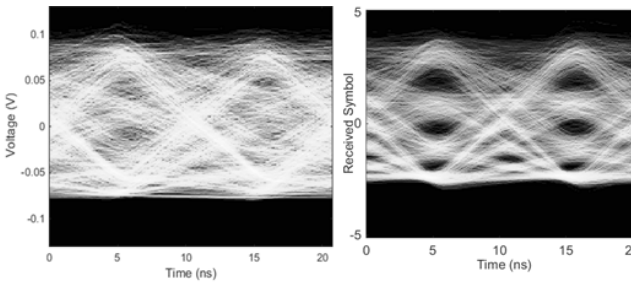

(a) (b)

Fig. 4. The eye diagrams before equalisation (a) and after equalisation (b) when 4 PAM is used to transmit 200 Mbps.

In this numerical method, the received signal $y(t)$ is expressed as

$$y(t) = h(t) * x(t) + n(t) \tag{6}$$

where $*$ is the convolution operator, $x(t)$ is the transmitted 4 PAM symbol, $h(t)$ is the overall channel response and $n(t)$ is additive noise within the system. In these simulations, the overall channel response $h(t)$ is obtained by convolving the temporal responses of the RCLED transmitter and the temporal response of the MPPC. Both of these temporal responses were modelled as an exponential decay,

$$h(t) = \frac{1}{T_C} e^{-\frac{t}{T_C}} \tag{7}$$

which means that they have an equivalent first order low-pass response with a bandwidth BW of

$$BW = \frac{1}{2*\pi*T_C} \tag{8}$$

where T_C is the equivalent of the RC time constant of a single pole RC filter. The MPPC has an output pulse width (90%-10%) of 10 ns, and this definition of the output pulse width means that the output pulse width is $2.2T_C$. This means that the SiPM has an effective T_C of 4.55 ns, which corresponds to a bandwidth of 35 MHz.

The modulation bandwidth of the RCLED is determined by the current density flowing through it and hence the applied bias voltage [17]. In 4 PAM, the effective bias voltage changes for different symbols and as a result, the modulation bandwidth of the RCLED changes at different symbol transitions. In particular, characterisation of the RCLED showed that over the bias range used to transmit 4 PAM data the bandwidth of the RCLED increases from 40 MHz to 137 MHz. Therefore, in the worst case scenario, the bandwidth of the RCLED is 40 MHz for all transitions. In contrast, in the best scenario the bandwidth of the RCLED for all the 4 PAM transitions is 137 MHz.

The ISI power penalty required to achieve a target BER of 10^{-3} at different RCLED bandwidths using the MPPC and 4 PAM to achieve a 200 Mbps when decision feedback equaliser (DFE) has been applied has been estimated. The DFE used has 10 feed forward taps and 5 feedback taps and the necessary tap coefficients were estimated using the least mean square (LMS) algorithm. A comparison of the estimated ISI penalty for the RCLED and for the RCLED with the MPPC shows that the ISI is dominated by the response of the MPPC module. Moreover, these results suggest that the power penalty required

for this system to maintain the target BER of 10^{-3} at 200 Mbps is expected to be between 2.9 and 3.4.

When the power levels needed to transmit 200 Mbps using 4 PAM were obtained experimental they corresponded to 43 photons per bit (13.1 aJ per bit) in the dark. Taking into account the reduced number of dark counts per bit arising from the higher data rate this meant that the average power penalty needed to overcome ISI in the dark was 3.13. The power levels needed to transmit 200 Mbps using PAM have also been determined in the presence of the ambient light level, 500 lux, recommended when work involves fine details. At this relatively high ambient light level 200 Mbps could be transmitted with 4 PAM using 177 photons per bit (53.9 aJ per bit). This corresponded to a power penalty in 500 lux of 3.37. Both these power penalties are consistent with the estimated power penalty. These results show that it is possible to estimate the impact of the finite width of output pulses on the signal levels needed to transmit data to a SiPM.

VI. METHODS TO INCREASE THE DATA RATE

Results in the previous section demonstrated that data rate of 200 Mbps can be achieved with a SiPM. However, SiPMs are a new, rapidly developing technology and these developments offer the prospect of achieving even higher data rates, for example 1Gbps.

One example of newer SiPMs are the recently released S13360 series manufactured by Hamamatsu. These devices have a PDP higher than 25% and the series includes arrays with three different pitches between individual SPADs (25 µm, 50 µm and 75 µm) and 3 total areas (1.69 mm^2, 9 mm^2 and 36 mm^2). However, according to the parameters listed in [18] the duration of the output pulses from devices in the S13360 series are several nanoseconds. Unfortunately, these devices will therefore suffer from inter-symbol interference (ISI) when OOK or 4-PAM are used to achieve data rates of 1 Gbps or higher. Estimates of the increase in power that will be required by the SiPM to support these higher data rates using OOK and 4-PAM have been obtained using the numerical method described in section V. In particular, assuming other components within the system have sufficient bandwidth, which may mean using a microLED[19] as the transmitter, (9) has been used to determine the power penalty required to overcome ISI at different ratios of the symbol rate to SiPM bandwidth.

The results of these calculations are shown as points in Fig. 5. In addition to the numerical results this figure shows curves that fit the two sets of data that are described by the equations

$$PP = \begin{cases} 1 & r_{sb} \le 1 \\ a.e^{br_{sb}} + c.e^{dr_{sb}} + k & 1 < r_{sb} < 2 \\ p1.r_{sb} + p2 & r_{sb} \ge 2 \end{cases} \quad (9)$$

where r_{sb} refers to the ratio of the symbol rate to the bandwidth of the SiPM The best fits to the two sets of results were obtaining using the parameters listed in table IV. If r_{sb}>5, so that p2 becomes smaller than the first term in the relevant equation, the power penalty needed to increase the data rate by increasing the symbol rate will be proportional to the increase in symbol rate.

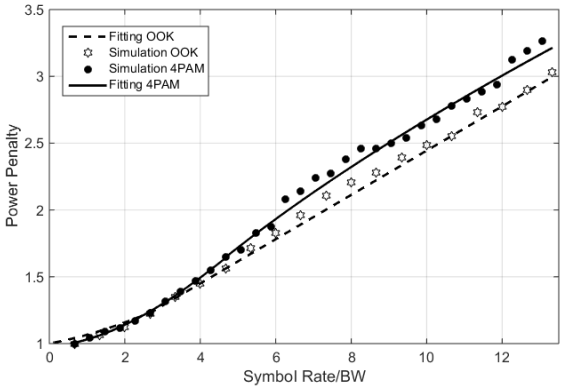

Fig.5. The estimated power penalty needed to employ DFE when the symbol period is shorter than the output pulse width.

Table IV: Fitting parameters of (9) used in Fig. 5

Fitted parameters	4-PAM	OOK
a	0.088	0.077
b	-1.38	-0.628
c	0.912	0.944
d	0.109	0.101
k	-0.01	-0.02
p1	0.19	0.17
p2	0.777	0.827

The bandwidth of the devices in the S13360 series are between 25 MHz and 58 MHz [18], which means that for OOK data rates of 300 Mbps or higher r_{sb}>5. This means that using DFE to increase the OOK data rate beyond 300 Mbps will incur an additional power penalty that is proportional to the increase in data rate, e.g. the number of photons per symbol needed to transmit 900 Mbps will be 3 times the same number needed to transmit 300 Mbps.

Rather than reducing the symbol time, and hence suffer ISI, an alternative approach to increasing the data rate is to retain the same symbol time but use higher orders of PAM[20]. In order to assess the practicality of this approach the method described in section III has been used to determine the number of detected photons needed to represent each level for different forms of PAM in the presence of different background counts per symbol.

Using 16 PAM and 32 PAM with the same symbol time as OOK increases the data rate by a factor of 4 and 5 respectively. Comparing the ratios in Table V to the additional power penalties incurred by reducing the symbol time for OOK to achieve the same increase in data rate, 4 and 5 respectively, shows that

Table V: The ratios of the average number of photons per symbol needed to transmit data using various levels of PAM to the average number of photons per symbol needed to transmit data using OOK.

Background counts per symbol	0.001	0.01	0.1	1	10	100
4 PAM	3.9	3.5	3.2	2.6	1.8	1.3
8 PAM	20.0	17.3	14.6	10.6	5.8	2.7
16 PAM	87.6	73.9	61.2	42.3	20.0	6.8
32 PAM	357.9	298.4	244.6	164.6	72.7	20.5

using these high levels of PAM is not a power efficient strategy. Similarly, the results in Table V show that tripling the data rate using 8 PAM is only worth considering at high background counts per symbol. This means that for these devices the two modulation schemes that are most useful are OOK and 4-PAM. However, 4-PAM should only be considered when operating with high numbers of background counts per symbol.

VII. METHOD OF PREDICTING RECEIVER SENSITIVITY

To support a data rate of 1 Gbps or higher using OOK the symbol time has to be less than or equal to 1 ns. According to the parameters listed in [18], symbol times of 1 ns or less are much shorter than the recovery time of the S13360 series. The recovery time determines the number of available SPADs within a SiPM and hence the effective PDE of the SiPM. For VLC applications, only count rates less than the maximum count are usable. As previously highlighted by the results in Fig 2 the paralyzable recovery time model can be used to calculate the effective PDE which is expressed as

$$PDE_{eff} = PDE_{max} \times \exp(-N_s/C_{max}eT) \qquad (10)$$

where PDE_{max} is the PDE of the SiPM listed in the relevant data sheet, N_s is the average number of SPADs fired within a symbol duration, T, and C_{max} is the maximum count rate of the device.

Another important factor needed to determine the sensitivity of a SiPM receiver is the background counts per symbol, which is a combination of dark counts and detected ambient light photons. The density of background photons per second incident on a 1 mm^2 detector from a range of lighting sources [21], each generating 500 lux of ambient light, has therefore been estimated. These estimates showed that a receiver will suffer from the minimum number of background photons when data is transmitted at wavelengths of approximately 410 nm. This suggests that these receivers should be used at these short wavelengths, where they also have a relatively high PDE. The combination of a band-pass filter 400FS40-50, which has a 40 nm bandwidth at 400 nm central wavelength and a 45% transmission, with a 24-degree FOV, means that a device with an active area of 1 mm^2 will typically experience 1.5×10^9 counts per second. In contrast the highest dark count rate for this series of devices is 7×10^5 counts per second per mm^2 and hence the dark count rate is negligible. This means that for a SiPM with an active area A and fill-factor FF, the number of detected background counts within a symbol time T can be calculated using

$$N_b = \frac{PDE}{FF} \times T \times A \times 1.5 \times 10^9 \qquad (11)$$

The other factors that determine the sensitivity of a SiPM receiver will be the maximum PDE, maximum count rate and bandwidth of the SiPM. SiPM devices that contain larger individual SPADs have a higher maximum PDE, but, smaller maximum count rates and bandwidths. To determine the significance of these competing factors the signal intensities required to transmit data to devices from the S13360 series using OOK have been estimated.

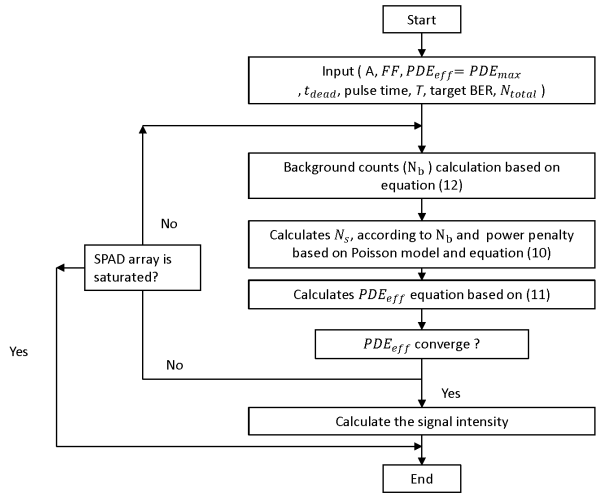

Fig.6. A general method to estimate the sensitivity of a SiPM.

A flow-chart representing the method used to estimate the signal intensity required by a SiPM to achieve a target BER, is shown in Fig 6. This method starts with the symbol time T, the target BER, the ambient light level and the specification of the SiPM of interest. The number of signal photons per symbol N_s is calculated using (9) and (11) and the Poisson model [11]. In the first iteration these calculations use the PDE for the SiPM from the data sheet. However, since during normal operation some SPADs in the SiPM will be recovering these results are used to estimate the effective PDE using (10). This effective PDE is then used to calculate better estimates of the number of background and hence signal counts per symbol. As long as the SiPM remains unsaturated this iterative process converges and so it is continued until the effective PDE becomes stable, which is defined as changed by less than 1%. Once the calculation converges the effective PDE and the number of signal photons per bit can be used to determine the power needed to transmit data at a particular rate in the specified ambient conditions.

VIII. PREDICTED PERFORMANCE WITH OOK

The method described in section VII has been used to estimate the optical signal intensity needed to transmit data to various devices from the S13360 series at different OOK data rates. Fig. 7 shows the estimated optical signal intensity needed to transmit OOK data to some SiPMs in this series with a BER of 10^{-3} in the presence of 500 lux (specifically 1.5×10^9 background counts per second per mm^2). As expected, the finite bandwidth of each type of SiPM means that the optical intensity needed to transmit data to it increases rapidly once the symbol rate is more than twice the bandwidth. Consequently, the maximum data rate that can be received by the SiPMs with the smallest number of SPADs is limited by their maximum count rate. Furthermore, these results confirm that, because the number of photons needed to transmit data in increasing levels of background light increases less rapidly than the number of detected background photons, see Fig. 3, SiPMs with the largest active areas are more sensitive. Overall, the results show that the best choice of SiPM is one with a large area containing small individual SPADs. In the case of the S13360 series this

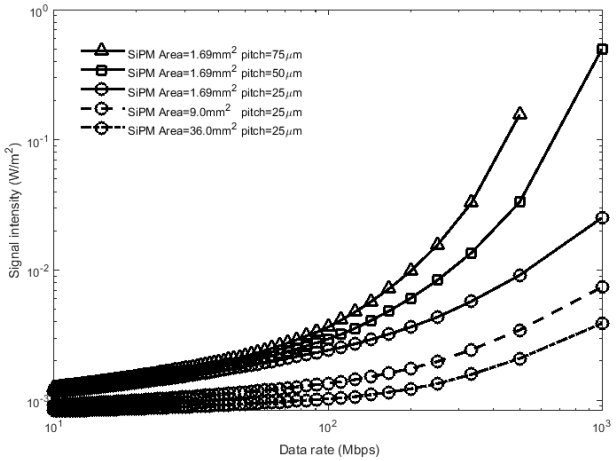

Fig.7. Signal intensities required by the SiPMs in S13360 series to achieve a BER of 10^{-3} in the 500 lux ambient light condition at different OOK data rates. In this figure the solid lines with different symbols represent the results from the devices in this series with the smallest total areas but different diameter SPADs whilst the lines with open circle symbols represent the SiPMs with the smallest diameter SPADs but different edge lengths and hence total areas.

means that the best choice of SiPM is the S13360-6025CS, which has an area of 36 mm^2 and a pitch of 25 μm.

The results in Fig. 7 show that the S13360-6025CS is expected to support 1 Gbps with a BER of 10^{-3} when the signal intensity is 4 mWm^{-2}. This data rate and BER have previously been achieved when a microLED, with a bandwidth of 833 MHz, was used as the transmitter and the receiver was a commercial PIN photodiode with a bandwidth of 1.4 GHz [19]. However, to achieve this data rate this receiver required more than 100 Wm^{-2}. When receiving 1 Gbps a future SiPM based receiver could therefore be at least 4 orders of magnitude more sensitive than a receiver containing a PIN photodiode.

Operating an ideal SiPM at higher data rates will require higher optical powers to maintain the same number of counts per bit. In addition, for these SiPMs increasing the data rate will increase the power penalty needed to overcome ISI. A combination these two effects and their maximum count rate will limit this generation of SiPMs to data rates of a few Gbps.

However, this is a new technology and future developments could significantly increase the achievable data rate. For example, integrating SiPMs with digital counters will result in a receiver with digital outputs which will not suffer from the ISI caused by the output pulses of the current device generation. When this type of SiPM device becomes commercially available it should be possible to support data rates of more than 10 Gbps.

IX. CONCLUSIONS

In this paper, it has been demonstrated that a 200 Mbps data rate can be achieved using a conventional SiPM in the VLC receiver under the typical ambient light condition. To the best of the authors knowledge this is the highest data rate achieved using this type of receiver in a VLC link operating in ambient light using 4 PAM.

In addition, to achieving this data rate this system has been used to highlight the importance of the maximum count rate of a SiPM when it is used in the receiver and to validate an efficient method of determining the signal levels needed to support PAM when the dominant noise source is shot (Poisson) noise. Most importantly, it has been used to validate methods to quantify the effects of important SiPM characteristics including the SPAD recovery time and the ISI caused by the finite width of the output pulses from this generation of SiPMs.

The additional power needed to increase data rates to S13360 series SiPMs beyond 300 Mbps by supporting PAM or reducing the OOK symbol time were compared. This comparison led to the conclusion that high levels of PAM are not a good means of achieving these higher data rates. In fact OOK is usually the best choice of modulation scheme for SiPM-based receivers.

The methods of quantifying the impact of various phenomena, validated in the paper, were then combined to create a method of determining the optical signal intensities needed to transmit data to SiPMs using OOK. The results showed that the best type of SiPM to use in receivers is one with a large total area containing small SPADs. In fact, with the best SiPM in the S13360 series it should be possible to transmit 1 Gbps with a transmitted optical power intensity that is 4 orders of magnitude smaller than the optical power intensity needed to achieve the same performance with a receiver containing a PIN photodiode. Further work is needed to confirm these predictions and to explore the possibility of achieving even higher data rates.

REFERENCE

[1] H. Haas, L. Yin, Y. Wang and C.Chen, "What is LiFi ?," *J. Light. Technol* ,vol. 34, no. 6, pp. 1533–1544,2016.

[2] T. Komine and M. Nakagawa "Fundamental analysis for visible light communication system using LED lights.," *IEEE Trans. Consum. Electron.*, vol. 50, no. 1, pp. 100–107, 2004.

[3] Ghassemlooy, Z., Alves, L. N., Zvanovec, S., & Khalighi, M. A. (Eds.). (2017). Visible light communications: theory and applications. CRC Press.

[4] E. Fisher, I. Underwood, and R. Henderson, "A reconfigurable 14-bit 60Gphoton/s Single-Photon receiver for visible light communications," *Eur. Solid-State Circuits Conf.*, pp. 85–88, 2012.

[5] D. Chitnis and S. Collins, "A SPAD-based photon detecting system for optical communications," *J. Light. Technol.*, vol. 32, no. 10, pp. 2028–2034, 2014.

[6] Y. Li, M. Safari, R. Henderson, and H. Haas, "Optical OFDM With Single-Photon Avalanche Diode," *IEEE Photonics Technol. Lett.*, vol. 27, no. 9, pp. 943–946, 2015.

[7] S. Gnecchi, N. A. W. Dutton, L. Parmesan, B. R. Rae, S. Pellegrini, S. J. Mcleod, L. A. Grant, and R. K. Henderson, "Analysis of Photon Detection Efficiency and Dynamic Range in SPAD-Based Visible Light Receivers," *J. Light. Technol* , vol. 34, no. 11, pp. 2774–2781, 2016.

[8] E. Fisher, I. Underwood, and R. Henderson, "A reconfigurable single-photon-counting integrating receiver for optical communications," *IEEE J. Solid-State Circuits*, vol. 48, no. 7, pp. 1638–1650, 2013.

[9] Kosman, J., Almer, O., Jalajakumari, A. V., Videv, S., Haas, H., & Henderson, R. K. (2016, July). 60 Mb/s, 2 meters visible light communications in 1 klx ambient using an unlensed CMOS SPAD receiver. In Photonics Society Summer Topical Meeting Series (SUM), 2016 IEEE (pp. 171-172). IEEE.

[10] D. Chitnis, L. Zhang, H. Chun, S. Rajbhandari, G. Faulkner, D. O'Brien, and S. Collins, "A 200 Mb / s VLC demonstration with a SPAD based receiver," in *IEEE SUM*, 2015,vol.3,pp. 226-227.

[11] Zhang L, Chitnis D, Chun H, et al. "A Comparison of APD-and SPAD-Based Receivers for Visible Light Communications" Journal of Lightwave Technology, 2018, 36(12): 2435-2442.

[12] Hamamastu, "S12571-010C",data sheet, December 2015

[13] Lee, Sang Hoon, and Robin P. Gardner. "A new G–M counter recovery time model." Applied Radiation and Isotopes 53.4-5 (2000): 731-737.

[14] A. Eisele, R. Henderson, B. Schmidtke, T. Funk, L. A. Grant, J. A. Richardson, and W. Freude, "185 MHz Count Rate, 139 dB Dynamic Range Single-Photon Avalanche Diode with Active Quenching Circuit in 130nm CMOS Technology," in. IISW, Japan, 2011, pp. 278–281.

[15] O. Almer, D. Tsonev, N. A. W. Dutton, T. Al Abbas, S. Videv, S. Gnecchi, H. Haas, and R. K. Henderson, “A SPAD-based Visible Light Communications Receiver Employing Higher Order Modulation,” *IEEE Global Telecommun.Conf*, 2015.
[16] J. G. Proakis, “Digital Communications,” *McGraw-Hill*, 2007.
[17] Schubert E F,“Light-emitting diodes[M]”, E. Fred Schubert, 2018.
[18] Hamamatsu, MPPCs for precision measurement, Aug. 2016.
[19] Ferreira R X G, Xie E, McKendry J J D, et al. High bandwidth GaN-basedmicro-LEDs for multi-Gb/s visible light communications. IEEE Photonics Technology Letters, 2016, 28(19): 2023-2026.
[20] Rajbhandari S, Chun H, Faulkner G E, et al. High-Speed Integrated Visible Light Communication System: Device Constraints and Design Considerations[J]. IEEE Journal on Selected Areas in Communications, 2015, 33(9): 1750-1757.
[21] M. Conner, “Light spectrum/spectrometer charts and raw data for commonlights," recommendation, Designing with LEDs, Jul. 2015.